

When confluent cells in culture are deprived of serum growth factors, the selective pathway of lysosomal proteolysis is activated (2, 3). To determine whether overexpression of human LGP96 affected this proteolytic pathway, we radiolabeled control CHO cells with [³H]leucine and transfected cells with [¹⁴C]leucine and then cultured both cell types on the same culture dishes to simultaneously follow degradation of ³H- and ¹⁴C-labeled proteins (14). Proteolysis was increased in the transfected cells, both in the presence and absence of serum, when compared with the control CHO cells (Fig. 4A). Similar results were obtained when control and transfected cells were analyzed in separate culture dishes (7). Cells that expressed half the amount of human LGP96 as the transfectants shown in Fig. 4A also showed half the increased protein degradation rates when compared to those in CHO cells, and cells transfected with plasmid containing no cDNA degraded proteins at rates similar to those of the untransfected control cells (7).

Several other aspects of the transfected cells were unaffected by overexpression of human LGP96. For example, the percentage of lysosomes broken during cell homogenization was similar in control and transfected cells (7), and [³H]RNase A was taken up by cells and digested within endosomes and lysosomes at normal rates (Fig. 4B). In addition, the cells grew at normal rates and had unaltered rates of protein synthesis (7). Finally, lysosomes isolated from human LGP96-overexpressing cells were more active in the *in vitro* uptake and degradation of [¹⁴C]GAPDH under all conditions tested (Fig. 4C).

Thus, overexpression of human LGP96 increased the activity of the selective lysosomal proteolytic pathway, and the level of LGP96 appears to be one rate-limiting component of the degradation machinery. It is not necessarily the only rate-limiting component, however, because overexpression of one protein may cause overexpression of interacting proteins (15). Whether LGP96 plays a role in the selective uptake of proteins by lysosomes, in addition to the binding of substrate proteins, remains to be studied.

REFERENCES AND NOTES

1. W. A. Dunn Jr., *Trends Cell Biol.* **4**, 139 (1994); S. A. Hayes and J. F. Dice, *J. Cell Biol.* **132**, 255 (1996).
2. H.-L. Chiang, S. R. Terlecky, C. P. Plant, J. F. Dice, *Science* **246**, 382 (1989); S. R. Terlecky, *Experientia (Basel)* **50**, 1021 (1994).
3. S. R. Terlecky and J. F. Dice, *J. Biol. Chem.* **268**, 23490 (1993).
4. F. Aniento, E. Roche, A. M. Cuervo, E. Knecht, *ibid.*, p. 10463; A. M. Cuervo, E. Knecht, S. R. Terlecky, J. F. Dice, *Am. J. Physiol.* **269**, C1200 (1995).
5. A. M. Cuervo, S. R. Terlecky, J. F. Dice, E. Knecht, *J. Biol. Chem.* **269**, 26374 (1994).
6. G. Schatz and B. Dobberstein, *Science* **271**, 1519 (1996).
7. A. M. Cuervo and J. F. Dice, unpublished results.
8. Y. Noguchiu *et al.*, *Biochem. Biophys. Res. Commun.* **164**, 1113 (1989).

9. Single-letter abbreviations for the amino acid residues are as follows: A, Ala; C, Cys; D, Asp; E, Glu; F, Phe; G, Gly; H, His; I, Ile; K, Lys; L, Leu; M, Met; N, Asn; P, Pro; Q, Gln; R, Arg; S, Ser; T, Thr; V, Val; W, Trp; and Y, Tyr.
10. Not all cultured cells express this selective lysosomal pathway of proteolysis. For example, skin fibroblasts show less of this activity than do lung fibroblasts, and certain transformed cell lines (such as COS cells) have no detectable activity (L. Terlecky, S. R. Terlecky, J. F. Dice, unpublished results).
11. M. Fukuda, J. Viitala, J. Matteson, S. R. Carlsson, *J. Biol. Chem.* **263**, 18920 (1988).
12. CHO cells were transfected with human LGP96 cDNA in the plasmid designated pCR-3 (Invitrogen, San Diego, CA) and selected for stable transfectants by resistance to Geneticin.
13. Hybridoma H4B4 was obtained from the Developmental Studies Hybridoma Bank maintained by the Department of Pharmacology and Molecular Sciences, Johns Hopkins University School of Medicine, Baltimore, MD, and the Department of Biological Sciences, University of Iowa, Iowa City, IA, under contract NO1-HD-6-2915 from the National Institute of Child Health and Human Development.
14. J. S. Auteri, A. Okada, V. Bochaki, J. F. Dice, *J. Cell. Physiol.* **115**, 159 (1983).
15. S. Gratzner *et al.*, *J. Cell Biol.* **129**, 25 (1995).
16. Binding assays were performed with the following procedure. Rat liver lysosomal membranes (100 µg of protein) prepared as described (4, 5) were immobilized in a nitrocellulose membrane after SDS-PAGE and incubated with RNase A (382 mM) or [¹⁴C]GAPDH (230 nM) in a renaturation buffer [50 mM tris-HCl (pH 7.5), 0.1 M potassium acetate, 0.15 M NaCl, 1 mM dithiothreitol (DTT), 5 mM MgCl₂, 1 mM EDTA, and 0.3% Tween 20] for 12 hours at 4°C. Bound protein was detected by ECL immunoblotting (Amersham International, Buckinghamshire, UK) with a specific antibody to RNase A (4, 5) or by direct exposure to a phosphor screen (Molecular Dynamics, Sunnyvale, CA). In other studies, rat liver lysosomal membrane proteins (2 mg) were solubilized in 20 mM tris-HCl (pH 7.5), 150 mM NaCl, and 1% Triton X-100 and then centrifuged at 100,000g for 30 min. The supernatant was incubated with GAPDH immobilized in a 2-ml Aminolink Plus gel column (Pierce, Rockford, IL) for 2 hours at 25°C. Flow through the column was collected, and after extensive washing, GAPDH-bound proteins were eluted with 10 ml of acetate buffer (pH 4.0) [25 mM sodium acetate (pH 4.0), 150 mM NaCl, 1 mM EDTA, 1 mM DTT, and 0.3% Tween 20] followed by 10 ml of 1 M NaCl in 0.1 M sodium phosphate buffer (pH 7.2).
17. Intracellular protein degradation in cultured fibroblasts was measured as described previously (14). Briefly, confluent cells were labeled with [³H]leucine or [¹⁴C]leucine for 20 hours at 37°C. After extensive washing, cells were trypsinized and replated in the presence of complete medium or serum-deprived medium. Aliquots of the medium were taken at the indicated times, and acid-soluble and -precipitable radioactivity was measured. Proteolysis was expressed as the percentage of precipitable radioactivity transformed to soluble radioactivity for each time. Proteolytic activity of isolated fibroblast lysosomes was measured by incubation of freshly isolated lysosomes (25 µg of protein) for 2 hours at 25°C with [¹⁴C]GAPDH (230 nM) in the *in vitro* degradation system (4, 5). In some assays, bovine brain cytosolic HSC73 (5 µg/ml) or 5 mM ATP and 5 mM MgCl₂ or both were added. Proteolysis was expressed as the percentage of the initial acid-precipitable radioactivity converted to acid-soluble radioactivity.
18. We thank M. Berne for the peptide sequencing. The polyclonal antibody to cathepsin D was a gift of G. Sahagian, Department of Physiology, Tufts University, Boston, MA. This research was funded by a Fundacion Ramon Areces (Spain) and American Liver Foundation postdoctoral fellowships and by NIH grant AG06116.

17 April 1996; accepted 7 June 1996

Lymphocyte Apoptosis: Mediation by Increased Type 3 Inositol 1,4,5-Trisphosphate Receptor

Adil A. Khan, Mark J. Soloski, Alan H. Sharp, Gabriele Schilling, David M. Sabatini, Shi-Hua Li, Christopher A. Ross, Solomon H. Snyder*

B and T lymphocytes undergoing apoptosis in response to anti-immunoglobulin M antibodies and dexamethasone, respectively, were found to have increased amounts of messenger RNA for the inositol 1,4,5-trisphosphate receptor (IP₃R) and increased amounts of IP₃R protein. Immunohistochemical analysis revealed that the augmented receptor population was localized to the plasma membrane. Type 3 IP₃R (IP₃R3) was selectively increased during apoptosis, with no enhancement of type 1 IP₃R (IP₃R1). Expression of IP₃R3 antisense constructs in S49 T cells blocked dexamethasone-induced apoptosis, whereas IP₃R3 sense, IP₃R1 sense, or IP₃R1 antisense control constructs did not block cell death. Thus, the increases in IP₃R3 may be causally related to apoptosis.

Calcium entry into cells appears to be a critical early event in apoptosis (programmed cell death) (1). In thymocytes,

A. A. Khan and D. M. Sabatini, Department of Neuroscience; M. J. Soloski, Department of Medicine; A. H. Sharp, G. Schilling, and S.-H. Li, Department of Psychiatry; C. A. Ross, Departments of Neuroscience and Psychiatry; and S. H. Snyder, Departments of Neuroscience, Psychiatry, and Pharmacology and Molecular Sciences, Johns Hopkins University School of Medicine, Baltimore, MD 21205, USA.

*To whom correspondence should be addressed.

apoptosis elicited by glucocorticoids is associated with a sustained increase in cytosolic calcium concentration, and depletion of calcium with chelating agents blocks apoptosis (2, 3). The endonuclease that causes characteristic apoptotic cleavage of chromatin is calcium-dependent (2, 4). Calcium entry also participates in cellular proliferation, especially in lymphocytes undergoing immune stimulation (5). The channels and mechanisms that account for the cellular

entry of calcium that mediates cellular proliferation and apoptosis have been difficult to identify. Although mature lymphocytes proliferate when subjected to immune stimuli, immature lymphocytes instead undergo apoptosis when stimulated in the same manner (2, 3).

The IP₃R may mediate calcium entry into lymphocytes and is localized on both the endoplasmic reticulum (ER) (6) and the plasma membrane (PM) (7). It cocaps with the T cell receptor-CD3 complex, which suggests that the IP₃R on T cells participates in the entry of calcium that initiates proliferative responses (8). At least three types of IP₃R, derived from three distinct genes, have been discriminated (9, 10). Although some differences in localization among these IP₃R subtypes have been observed (9, 10), functional differences have not yet been uncovered.

Here, we investigated whether IP₃R are critical for lymphocyte apoptosis. In response to immune stimuli, mature B lymphocytes undergo proliferation and antibody formation, whereas immature B lymphocytes die by an apoptotic process (2, 3, 11). The WEHI-231 cell line was derived from a phenotypically B cell lymphoma and undergoes apoptosis when stimulated by antibodies to immunoglobulin M (anti-IgM) (11). We examined the distribution of IP₃R on WEHI-231 cells treated with anti-IgM. Flow cytometric analysis showed that the apoptotic cells have increased granularity, which is reflected as an increase in side light scatter; the cellular shrinkage and fragmentation results in a decrease in forward light scatter (12) (Fig. 1A). An antiserum that recognizes all IP₃R sub-

types revealed a homogeneous population of staining in the dead cell population, with a mean fluorescence intensity an order of magnitude greater than the negligible staining evident in live and unstimulated control cells (Fig. 1, B and C).

IP₃R staining in the dead cells was restricted to the area of the PM (Fig. 1D). Because all of the cells still excluded trypan blue, they were intact and should not admit antibody molecules to the interior. Thus, the staining

presumably represented the external PM surface of the cells. The antiserum was specific; immunoblot analysis revealed a single discrete band at 260 kD (Fig. 1E). The intensity of this band for extracts of dead WEHI-231 cells was six times that for live cells (Fig. 1E). We used Northern blot analysis to monitor mRNA for the three subtypes of IP₃R in WEHI-231 cells in which apoptosis was initiated by anti-IgM (13). IP₃R2 mRNA was not detected, IP₃R1 mRNA amounts were similar to those in con-

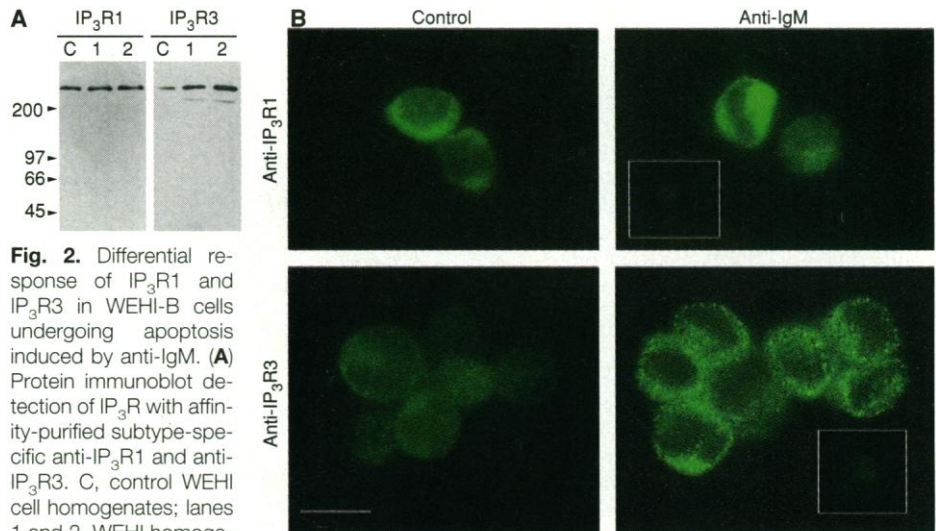
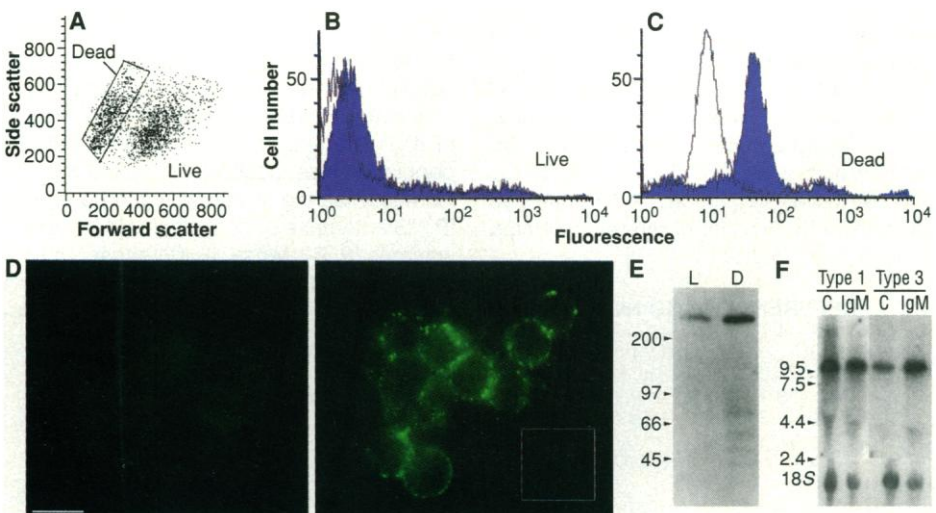


Fig. 2. Differential response of IP₃R1 and IP₃R3 in WEHI-B cells undergoing apoptosis induced by anti-IgM. **(A)** Protein immunoblot detection of IP₃R with affinity-purified subtype-specific anti-IP₃R1 and anti-IP₃R3. C, control WEHI cell homogenates; lanes 1 and 2, WEHI homogenates after 24 and 48 hours, respectively, of anti-IgM exposure. **(B)** Fluorescence microscopy of WEHI cells undergoing apoptosis. WEHI cell suspensions in HBSS, 1 mM HEPES, and fetal bovine serum (FBS) (2%) were fixed, permeabilized (14), and stained with subtype-specific anti-IP₃R1 and anti-IP₃R3 before and after 48 hours of exposure to anti-IgM. Insets: WEHI cells, after exposure to anti-IgM, were stained with anti-IP₃R1 and anti-IP₃R3 that had been blocked with an excess of IP₃R1 peptide and IP₃R3 peptide, respectively. Results are from a representative experiment. Scale bar, 10 μ m. Each experiment was done three times with similar results.

Fig. 1. Apoptotic WEHI B cells display enhanced IP₃R immunoreactivity on their PM. **(A)** WEHI-231 cell suspensions were analyzed for forward versus side light scatter after 48 hours of exposure to anti-IgM. **(B and C)** Flow cytometric analysis of WEHI cells undergoing apoptosis. WEHI cell suspensions in Hanks' balanced salt solution (HBSS), 1 mM HEPES, and FBS (2%) were stained with affinity-purified anti-IP₃R after 48 hours of exposure to anti-IgM. WEHI cells were electronically gated from the live (B) and dead (C) populations in (A). Open curve, background control cells stained with nonspecific rabbit immunoglobulin G and goat antibodies to rabbit fluorescein isothiocyanate (FITC); blue curve, cells stained with affinity-purified anti-IP₃R and the same antibodies to FITC. **(D)** Localization of IP₃R surface antigens by immunofluorescence. WEHI-231 cell suspensions were stained with affinity-purified anti-IP₃R before and after 48 hours of exposure to anti-IgM. Inset: After exposure to anti-IgM, WEHI-231 cells were stained with anti-IP₃R blocked with an excess of purified IP₃R. Scale bar, 10 μ m. **(E)** Protein immunoblot detection of IP₃R with affinity-purified anti-IP₃R. Live versus dead populations were electronically gated as in (B) and (C) and sorted for protein immunoblot analysis after 48 hours of stimulation with anti-IgM. L and D, live and dead WEHI cells; molecular masses are shown at the left (in kilodaltons). **(F)** Detection of IP₃R subtype by Northern blot analysis for mRNA in WEHI cells undergoing apoptosis. C, control WEHI cells; IgM, WEHI cells after 24 hours of treatment with anti-IgM. Type 1 and type 3 refer to oligonucleotide probes specific for IP₃R1 and IP₃R3, respectively. An 18S RNA probe was used as a control for the quantity of RNA. Results are from a representative experiment. Protein immunoblots and Northern blots were quantified on a digital scanner. All experiments were done three times with similar results.



control cells, and IP₃R3 mRNA amounts were three to five times those in controls (Fig. 1F).

Antibodies to unique cytoplasmic do-

main of IP₃R3 and IP₃R1 (14) revealed IP₃R3 protein amounts associated with apoptosis that were 10 times those in con-

control cells, whereas IP₃R1 protein amounts were similar in control and apoptotic cells (Fig. 2A). Permeabilized anti-IgM-treated

Fig. 3. Protein immunoblot detection of IP₃R with affinity-purified subtype-specific anti-IP₃R1 and anti-IP₃R3. **(A)** Increase of IP₃R3 in apoptotic thymocytes. Thymocytes cultured in RPMI 1640 with FBS (10%) were incubated with 0.1 μM dexamethasone for 3, 6, or 12 hours and stained with anti-IP₃R; C, control thymocytes. Upper panel, protein immunoblot analysis with anti-IP₃R1; lower panel, IP₃R1 blot stripped and reprobed with anti-IP₃R3. We primarily detected a 220-kD IP₃R3 band in thymus tissue preparations; this size is in accordance with our observations in other tissue preparations relating to the sensitivity of the IP₃R to proteolysis. A 200-kD molecular mass marker is shown at the left. **(B)** Increase of IP₃R3 in apoptotic S49 cells. Cells were incubated with 10 nM dexamethasone for 24, 48, or 72 hours; C, control S49 cell homogenates. Upper panel, anti-IP₃R1; lower panel, anti-IP₃R3. **(C)** Fluorescence microscopy of thymocytes undergoing apoptosis. Thymocyte cell suspensions in HBSS, 1 mM HEPES, and FBS (2%) were fixed, permeabilized, and stained with affinity-purified subtype-specific anti-IP₃R1 and anti-IP₃R3 before and after 12 hours of exposure to 0.1 μM dexamethasone. Insets: Thymocytes were stained with anti-IP₃R1 and anti-IP₃R3 that had been blocked with an excess of IP₃R1 peptide and IP₃R3 peptide, respectively. Results are from a representative experiment. Scale bar, 10 μm. **(D and E)** Fluorescence microscopy of thymocytes and S49 cells undergoing apoptosis. Cells were fixed, permeabilized, and stained with affinity-purified subtype-specific anti-IP₃R1 and anti-IP₃R3 before and after exposure to dexamethasone. In (D), the upper panel shows the diffuse nature of anti-IP₃R1 staining in the control thymocytes; the lower panel shows the punctate nature of anti-IP₃R3 staining in thymocytes after 12 hours of exposure to 0.1 μM dexamethasone. In (E), S49 cells were stained with anti-IP₃R1 and anti-IP₃R3 before and after 72 hours of exposure to 10 nM dexamethasone. Scale bar, 10 μm. Each experiment was done three times with similar results.

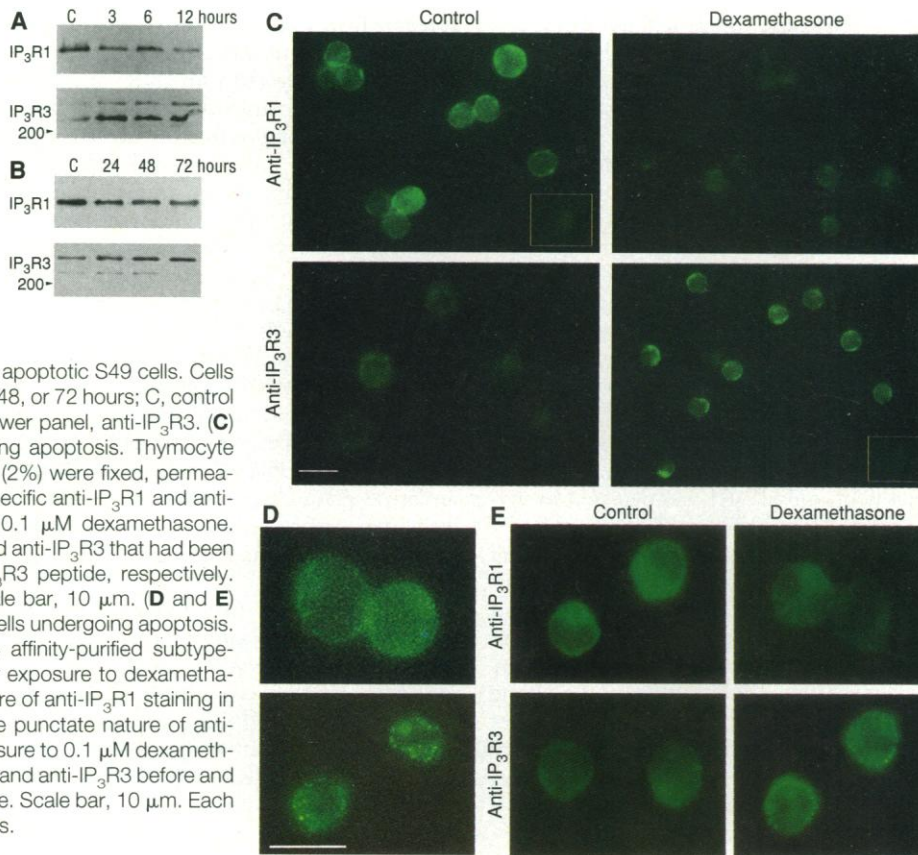
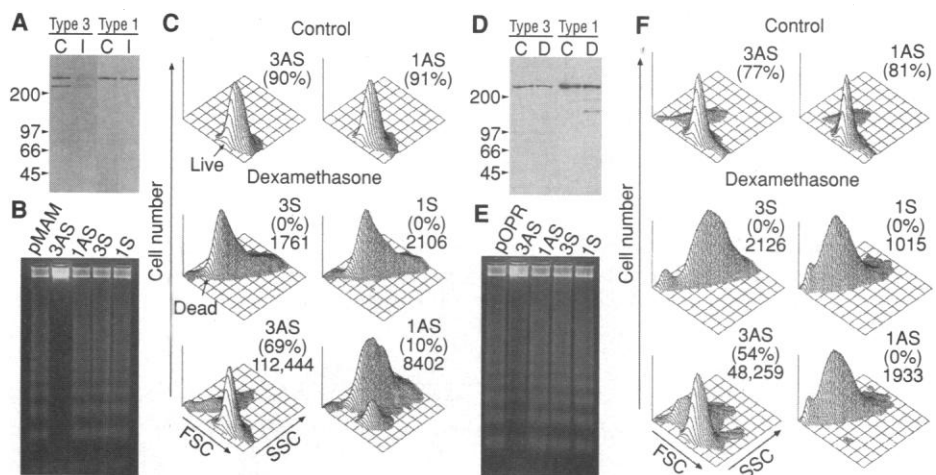


Fig. 4. IP₃R3 antisense DNA transfection blocks lymphocyte death. **(A)** Protein immunoblot detection of IP₃R in S49 cells transfected with dexamethasone-inducible IP₃R3 antisense before (C) and 7 days after (I) induction of plasmids by 10 nM dexamethasone. Type 3, protein immunoblot analysis with anti-IP₃R3; type 1, IP₃R3 blot stripped and reprobed with anti-IP₃R1. Molecular mass markers are shown at the left (in kilodaltons). **(B)** Agarose gel electrophoresis of DNA isolated from S49 cells transfected with dexamethasone-inducible plasmids containing 5' portions of IP₃R3 and IP₃R1 in sense and antisense orientations after 4 days of exposure to 10 nM dexamethasone. pMAM, S49 cells transfected with plasmid alone; 3AS, 1AS, 3S, and 1S refer to S49 cells transfected with plasmids containing IP₃R3 antisense, IP₃R1 antisense, IP₃R3 sense, and IP₃R1 sense, respectively. **(C)** Forward versus side light scatter (FSC versus SSC) of S49 cells as assessed by flow cytometry after 7 days of exposure to 10 nM dexamethasone. S49 cells were transfected with dexamethasone-inducible plasmids containing 5' portions of IP₃R3 and IP₃R1 in antisense or sense orientations; 10,000 cells were analyzed in each condition. The percentage of live cells in each cell line is indicated in parentheses; [³H]thymidine counts reflecting relative amounts of DNA synthesis are shown below these percentages. Results are from a representative experiment. **(D)** Protein immunoblot detection of IP₃R in S49 cells transfected with constitutively expressed IP₃R3 antisense before (C) and 4 days after (D) treatment with 0.1 μM dexamethasone. Type 3, protein immunoblot analysis with anti-IP₃R3; type 1, IP₃R3 blot stripped and reprobed with anti-IP₃R1. **(E)** Agarose gel electrophoresis of DNA isolated from S49 cells transfected with constitutively expressing plasmids containing 5' portions of IP₃R3 and IP₃R1 in sense and antisense orientations after 2 days of exposure to 0.1 μM dexamethasone. pOPR, S49 cells transfected with plasmid alone. **(F)** Forward versus side light scatter of S49 cells as assessed by flow cytometry after 4 days of exposure to 0.1 μM dexamethasone. Results are from a representative experiment. These experiments were done three times with similar results. Standard deviations for the mean counts per minute in (C) and (F) are 1474, 1901, 4943, and 12,087 for pMAM 3S, 1S, 1AS, and 3AS, respectively, and 840, 520, 2030, and 12,573 for pOPR 3S, 1S, 1AS, and 3AS, respectively.



cells displayed a punctate distribution of IP₃R immunoreactive staining along the region of the PM. In contrast, no increase in staining was evident with anti-IP₃R1, and intracellular staining was diffuse (Fig. 2B).

To determine the generality of the correlation of increased IP₃R with apoptosis, we treated rat thymocytes and murine S49 thymoma cells with dexamethasone (15, 16). The S49 cell line is highly sensitive to killing by glucocorticosteroids and has been extensively studied as a model for steroid-induced apoptosis (17). In thymocytes and S49 cells treated with dexamethasone, the amounts of IP₃R were 20 times and 5 times, respectively, those in controls; IP₃R1 decreased in both cell types (Fig. 3, A and B). The IP₃R2 in thymocytes and S49 cells decreased in both cell types after dexamethasone treatment (18). Immunohistochemical analysis corroborated these findings (Fig. 3, C to E). Before dexamethasone treatment, only IP₃R1 was detected in thymocytes. After 12 hours of dexamethasone treatment, IP₃R1 staining decreased and IP₃R3 immunoreactivity in a second population of smaller cells was increased, with a punctate distribution along the PM. These results fit with the known greater sensitivity to glucocorticoid-induced apoptosis of the smaller, more immature cortical thymocytes relative to that of the larger, more mature medullary cells (15, 19). In thymic sections, IP₃R3 immunostaining was faint in control thymocytes but increased in cortical thymocytes after the rats received intraperitoneal injections of dexamethasone; no staining was observed in medullary regions (18).

To determine the functional relation between elevations in IP₃R and apoptosis, we constructed plasmids containing 5' portions of IP₃R3 and IP₃R1 in sense and antisense orientations (20). Stably transfected cell lines were obtained by introducing dexamethasone-inducible and constitutively expressing plasmids into the T cell thymoma S49. Apoptosis was evoked by treatment with dexamethasone, which is well known to cause growth

arrest and inhibit proliferation of S49 cells (17). With either inducible or constitutive plasmids, cells expressing IP₃R3 antisense were protected from glucocorticoid-induced apoptosis (Fig. 4, B, C, E, and F) as monitored by light scatter analysis, [³H]thymidine incorporation (21), and DNA fragmentation (17). Cells transfected with IP₃R3 sense and IP₃R1 antisense constructs were not protected and underwent growth arrest and morphological changes associated with apoptosis. IP₃R3 antisense protection against apoptosis was associated with an inhibition of the five-fold dexamethasone-induced increases in the amount of IP₃R3 protein in apoptotic cells (Fig. 4, A and D). Dexamethasone-treated S49 control cells undergoing apoptosis showed increases in intracellular calcium concentration [Ca²⁺]_i levels that were associated with alterations in light scatter (Fig. 5) (22). Transfections with either dexamethasone-inducible or constitutive IP₃R3 antisense plasmids prevented these [Ca²⁺]_i elevations, whereas IP₃R3 sense, IP₃R1 sense, or IP₃R1 antisense control plasmids did not.

Our data show that transfection with IP₃R3 antisense constructs selectively prevents lymphocyte apoptosis and that interference with apoptosis may result from decreased calcium entry in the IP₃R3 antisense-expressing cell lines, inhibition of signaling pathways specific for IP₃R3, or both. These findings imply a causal role for IP₃R3 in lymphocyte apoptosis and also indicate a possible mechanism for apoptosis, namely augmentation of Ca²⁺ entry through IP₃R3 Ca²⁺ channels in the PM. Our results support other evidence for a major role of Ca²⁺ entry in apoptosis (2, 3, 16) and suggest an interesting dichotomy between IP₃R subtypes that may explain how calcium can promote such opposed cellular functions as proliferation and death.

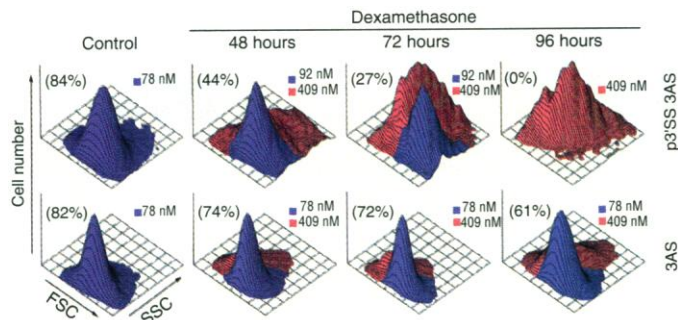
The localization of newly expressed IP₃R to the PM in apoptotic lymphocytes, as well as the selective up-regulation of IP₃R3 in these cells, implies that the population of

IP₃R3 associated with apoptosis is localized to the PM, where it might regulate capacitative Ca²⁺ entry (23). In unstimulated lymphocytes, antibodies directed to the cytoplasmic domain of IP₃R3 also stained the ER and nuclear membrane (18). Bell and associates (9) also observed IP₃R3 staining of the ER and the nuclear membrane of COS cells. IP₃R3 is also selectively augmented in dorsal root ganglion cells undergoing cell death induced by deprivation of nerve growth factor, which suggests a similar role for IP₃R3 in neuronal apoptosis (18). A selective association of IP₃R3 with calcium entry into apoptotic lymphocytes suggests that drugs blocking IP₃R3 but not IP₃R1 could inhibit apoptosis without disrupting calcium release mediated by IP₃R1 in the ER. Such drugs might have therapeutic relevance in conditions associated with apoptosis, such as the loss of CD4⁺ lymphocytes in acquired immunodeficiency syndrome (24).

REFERENCES AND NOTES

1. J. F. R. Kerr, A. H. Wyllie, A. R. Currie, *Br. J. Cancer* **26**, 239 (1972); A. H. Wyllie, *Nature* **284**, 555 (1980).
2. N. Kaiser and I. S. Edelman, *Proc. Natl. Acad. Sci. U.S.A.* **74**, 638 (1977).
3. D. J. McConkey, P. Hartzell, J. F. Amador-Perez, S. Orrenius, S. M. Jondal, *J. Immunol.* **143**, 1801 (1989); D. J. McConkey, S. Orrenius, M. Jondal, *Immunol. Today* **11**, 120 (1990); P. Nicotera, G. Bellomo, S. Orrenius, *Annu. Rev. Pharmacol. Toxicol.* **32**, 449 (1992).
4. J. N. Vanderbilt, K. S. Bloom, J. N. Anderson, *J. Biol. Chem.* **257**, 13009 (1982); J. J. Cohen and R. C. Duke, *J. Immunol.* **132**, 38 (1984); H. Kizaki, T. Tadakuma, C. Odaka, J. Muramatsu, Y. Ishimura, *ibid.* **143**, 1790 (1989).
5. J. F. Whitfield and T. Youdale, *Exp. Cell Res.* **43**, 602 (1966); G. L. Asherson, M. J. Davey, P. J. Goodford, *J. Physiol. (London)* **206**, 32 (1970); A. Weiss, J. Imboden, D. Schoback, J. Stobo, *Proc. Natl. Acad. Sci. U.S.A.* **81**, 4169 (1984); A. Weiss et al., *Annu. Rev. Immunol.* **4**, 593 (1986); M. A. Goldsmith and A. Weiss, *Science* **240**, 1029 (1988); R. S. Lewis and M. D. Cahalan, *Annu. Rev. Immunol.* **13**, 623 (1995).
6. M. J. Berridge and R. F. Irvine, *Nature* **341**, 197 (1989); C. A. Ross et al., *ibid.* **339**, 468 (1989); H. Otsu, A. Yamamoto, N. Maeda, K. Mikoshiba, Y. Tashiro, *Cell Struct. Funct.* **15**, 163 (1990); S. K. Joseph, A. P. Thomas, R. J. Williams, R. F. Irvine, J. R. Williamson, *J. Biol. Chem.* **259**, 3077 (1984); H. Streb, E. Bayerdorffer, W. Haase, R. Irvine, I. Schulz, *J. Membr. Biol.* **81**, 241 (1984); D. M. Deffert, S. Hill, H. A. Pershadsingh, W. R. Sherman, J. M. McDonald, *Biochem. J.* **236**, 37 (1986); J. P. Lievreumont, A. M. Hill, M. Hilly, J. P. Mauger, *ibid.* **300**, 419 (1994).
7. M. Kuno and P. Gardner, *Nature* **326**, 301 (1987); G. Guillemette, T. Balla, A. J. Baukal, K. J. Catt, *J. Biol. Chem.* **263**, 4541 (1988); R. Penner, G. Matthews, E. Neher, *Nature* **334**, 499 (1988); P. Gardner, *Annu. Rev. Immunol.* **8**, 231 (1990); D. Restrepo, T. Miyamoto, B. P. Bryant, J. H. Teeter, *Science* **249**, 1166 (1990); A. A. Khan, J. P. Steiner, S. H. Snyder, *Proc. Natl. Acad. Sci. U.S.A.* **89**, 2849 (1992); T. Fujimoto, S. Nakade, A. Miyawaki, K. Mikoshiba, K. Ogawa, *J. Cell Biol.* **119**, 1507 (1992); D. A. Fadool and B. W. Ache, *Neuron* **9**, 907 (1992); A. H. Sharp, S. H. Snyder, S. K. Nigam, *J. Biol. Chem.* **267**, 7444 (1992); L. Feng, B. Pereira, N. Kraus-Friedman, *Cell Calcium* **13**, 79 (1992); A. M. Cunningham et al., *Neuroscience* **57**, 339 (1993); M. Kuno, N. Maeda, K. Mikoshiba, *Biochem. Biophys. Res. Commun.*

Fig. 5. Forward versus side light scatter of S49 p3'SS 3AS and 3AS cells as assessed by flow cytometry before and after 2, 3, and 4 days of exposure to 0.1 μM dexamethasone. p3'SS refers to S49 cells with the constitutively expressing IP₃R3 antisense plasmid turned off; 3AS refers to S49 cells constitutively expressing IP₃R3 antisense. The percentages of live cells in each cell line are indicated in parentheses. [Ca²⁺]_i values for live (blue) and dead (red) populations of cells are indicated in brackets; 10,000 cells were analyzed in each condition. Each experiment was done three times with similar results.



- 199, 1128 (1994); M. Mayrlleitner, R. Schafer, S. Fleischer, *Cell Calcium* **17**, 141 (1995).
8. A. A. Khan, J. P. Steiner, M. G. Klein, M. F. Schneider, S. H. Snyder, *Science* **257**, 815 (1992).
 9. O. Blondell, J. Takeda, H. Janssen, S. Seino, G. Bell, *J. Biol. Chem.* **268**, 11356 (1993).
 10. T. C. Sudhof, C. L. Newton, B. T. Archer III, Y. A. Ushkaryov, G. A. Mignery, *EMBO J.* **10**, 3199 (1991); C. A. Ross, S. K. Danoff, M. J. Schell, S. H. Snyder, A. Ullrich, *Proc. Natl. Acad. Sci. U.S.A.* **89**, 4265 (1992).
 11. N. L. Warner, A. W. Harris, G. A. Gutman, in *Membrane Receptors of Lymphocytes*, M. Seligmann, J. L. Preud'homme, F. M. Kourilsky, Eds. (North-Holland, Amsterdam, 1975), p. 203; A. DeFranco, M. Davis, W. E. Paul, in *B and T Cell Tumors: Biological and Clinical Aspects*, E. Vitetta, Ed. (Academic Press, New York, 1982), pp. 445–450; D. W. Scott, A. O'Garra, D. Warren, G. G. B. Klaus, *J. Immunol.* **139**, 3924 (1987); A. W. Boyd and J. W. Schrader, *ibid.* **126**, 2466 (1981); L. E. Benhamou, P.-A. Casenave, P. Sarthou, *Eur. J. Immunol.* **20**, 1405 (1990); J. Hasbold and G. G. B. Klaus, *ibid.*, p. 1685.
 12. C. Dive *et al.*, *Biochim. Biophys. Acta* **1133**, 275 (1992); Z. Darzynkiewicz *et al.*, *Cytometry* **13**, 795 (1992).
 13. Probes were inserts from plasmid subclones derived from a mouse placenta cDNA library (IP₃R1, AGTCT-TATTGTCAAAGCTTGCCCTTCCAAAGCCGCGAGATGAAGCA; IP₃R2, TTTCAACCAGCCACGATGGACAGTCAGTGTGTGAGACAAG; IP₃R3, CACTCCATCTGTCCCCACTACATGTGCCATAAA-TGTGGCAGCT). Total RNA was extracted from cells, and each lane contained ~25 µg of total RNA. An 18S RNA probe was used to normalize the quantity of the RNA.
 14. Antibodies to synthetic IP₃R peptides were prepared essentially as described [E. Harlow and D. Lane, *Antibodies, A Laboratory Manual* (Cold Spring Harbor Laboratory, Cold Spring Harbor, NY, 1988)]. Rabbit antibodies to the COOH-terminal amino acids of rat IP₃R1, IP₃R2, and IP₃R3—residues 2736 to 2749 (GHPPHM-NVNPQQPA), 2688 to 2701 (GSNTPHVNHHMPPH), and 2655 to 2670 (RRQLGFVDVQNCMSR), respectively—were prepared. An internal anti-IP₃R, residues 2432 to 2444 (VSEVSVPEILEED), was also used with similar results. Most of the ER IP₃R is cytoplasmic, with membrane-spanning loop regions in the lumen of the ER. A similar structure presumably exists in the IP₃R of the PM, with only a small region of the protein exposed extracellularly. As expected if the COOH-terminus of the putative PM IP₃R is cytoplasmic, no staining was observed in unpermeabilized cells. Accordingly, cells were permeabilized before staining with subtype-specific anti-IP₃R. Abbreviations for the amino acid residues are as follows: A, Ala; C, Cys; D, Asp; E, Glu; F, Phe; G, Gly; H, His; I, Ile; K, Lys; L, Leu; M, Met; N, Asn; P, Pro; Q, Gln; R, Arg; S, Ser; T, Thr; V, Val; W, Trp; and Y, Tyr.
 15. X. M. Sun, D. Dinsdale, R. T. Snowden, G. M. Cohen, D. N. Skilleter, *Biochem. Pharmacol.* **44**, 2131 (1992).
 16. D. J. McConkey *et al.*, *Arch. Biochem. Biophys.* **269**, 365 (1989); J. J. Cohen, *Semin. Immunol.* **4**, 363 (1992).
 17. A. W. Harris, *Exp. Cell Res.* **60**, 341 (1970); P. Ralph, R. Hyman, R. Epstein, I. Nakoinz, M. Cohn, *Biochem. Biophys. Res. Commun.* **55**, 1085 (1973); J. M. Harmon, M. R. Norman, B. J. Fowlkes, E. B. Thompson, *J. Cell. Physiol.* **98**, 267 (1979); W. V. Vedecis and H. D. Bradshaw Jr., *Mol. Cell. Endocrinol.* **30**, 215 (1983); M. Danielson, D. O. Peterson, M. R. Stallcup, *Mol. Cell. Biol.* **3**, 1310 (1983); L. M. Caron-Leslie and J. A. Cidlowski, *Mol. Endocrinol.* **5**, 1169 (1991).
 18. A. A. Khan and S. H. Snyder, unpublished data.
 19. I. Screpanti *et al.*, *J. Immunol.* **142**, 3378 (1989); C. D. Surh and J. Sprent, *Nature* **372**, 100 (1994).
 20. The polymerase chain reaction (PCR) was used to create DNA fragments corresponding to positions -81 to +9 of IP₃R1 and IP₃R3 mRNA. This region spans the translation initiation start site and shares no homology between the two receptors. An upstream primer (IP₃R1, AAGGAAGCTAGCGGCGCGACTACAAAGGATTGCA; IP₃R3, AAGGAAGCTAGCGGCGCGAGCGCGCTCAGTCTCT) and a downstream primer (IP₃R1, AAGGAAGCTAGCGGCGCGGACTACAAAGGATTGCA; IP₃R3, AAGGAAGCTAGCGGCGCGCTCAGCGAGGCTTGGC) were used in a PCR. As templates for the IP₃R3 and IP₃R1 antisense and sense constructs, cDNA for the IP₃R3 and rat brain cDNA for the IP₃R1 were used, respectively. For creation of the constitutive constructs, the amplified DNA fragments were digested with Not I and subcloned into pOPRSVI (Stratagene) that had been linearized with the same enzyme. pOPRSVI is part of the LacSwitch Inducible Mammalian Expression System. The constitutive expression of pOPRSVI was turned off by cotransfection of the eukaryotic Lac repressor-expressing vector p3'SS. Several clones were analyzed by DNA sequencing to identify constructs with inserts in the antisense and sense orientations. The dexamethasone-inducible constructs were prepared in the same fashion except that the amplified DNA fragments and vector pMAMneo (Clontech) were digested with Nhe I. Dexamethasone treatment activated expression of IP₃R3 antisense in the dexamethasone-inducible pMAM plasmid constructs and inhibited dexamethasone-induced increases in IP₃R3 protein (Fig. 4A). In the dexamethasone-inducible IP₃R3 antisense-transfected cells, immunoblot analysis with antiserum to IP₃R3 revealed a reduction in amounts of IP₃R3 protein relative to noninduced control cells, whereas amounts of IP₃R1 in control and dexamethasone-treated IP₃R3 antisense cells were similar (Fig. 4A). S49 cells constitutively expressing IP₃R3 antisense had low resting amounts of IP₃R3 that did not increase with dexamethasone exposure.
 21. Relative amounts of DNA synthesis were measured in transfected cell lines after dexamethasone treatment by culturing 10⁵ cells in 0.5 ml of medium with 1 µCi of [³H]thymidine. After 18 hours, cells were lysed onto glass filters for scintillation counting. DNA synthesis data represent the mean counts per minute ± SD for triplicate determinations and are representative of four experiments. DNA synthesis was measured after 4 days of incubation in 10 nM dexamethasone for cell lines transfected with the dexamethasone-inducible plasmid pMAM and after 2 days of incubation in 0.1 µM dexamethasone for cell lines transfected with the constitutively expressing plasmid pOPRSVI.
 22. Transfected S49 cells in culture medium (RPMI 1640 containing 10% heat-inactivated FBS), either untreated or treated with 0.1 µM dexamethasone for 2, 3, or 4 days, were loaded with 2 µM Indo-1 AM (Molecular Probes) by incubation for 45 min at 37°C in 145 mM NaCl, 5 mM KCl, 0.1 mM MgCl₂, 1 mM CaCl₂, 5.5 mM glucose, and 15 mM Hepes (pH 7.5). Indo-1 fluorescence was analyzed with a FACStarplus flow cytometer (Becton Dickinson). The fluorescence data were converted to [Ca²⁺]_i values [P. S. Rabinovitch, C. H. June, A. Grossmann, J. A. Ledbetter, *J. Immunol.* **137**, 952 (1986)]. Electric grays were drawn to separate live and dead cells. The use of blue and red to indicate cells containing low and high calcium concentrations was based on lines of demarcation between live and dead populations of cells that most clearly resolved the low-calcium (78 nM) and high-calcium (409 nM) groups of cells, and it highlights the association between changes in light scatter and increases in [Ca²⁺]_i after dexamethasone treatment. Loss of membrane integrity occurs late in apoptosis. [Ca²⁺]_i measurement in cells with changes in light scatter reflects only those cells whose membrane integrity was still intact and excluded trypan blue.
 23. J. W. Putney Jr., *Cell Calcium* **7**, 1 (1986); R. S. Lewis and M. D. Cahalan, *Cell Regul.* **1**, 99 (1989).
 24. L. Meynard *et al.*, *Science* **257**, 217 (1992); M. L. Gougeon and L. Montagnier, *ibid.* **260**, 1269 (1993); C. J. Li, D. J. Friedman, C. Wang, V. Metelev, A. B. Pardee, *ibid.* **268**, 429 (1995).
 25. We thank G. Bell for IP₃R3 cDNA and C. Williams for pathology photography. Supported by the W. C. Keck Foundation and by USPHS grants AI-20922 and AI-37934 (to M.J.S.), MH43040 (to C.A.R.), and MH-18501 and Research Scientist Award DA-00074 (to S.H.S.).

21 December 1995; accepted 29 April 1996

The POU Factor Oct-6 and Schwann Cell Differentiation

Martine Jaegle, Wim Mandemakers, Ludo Broos, Ronald Zwart, Alar Karis, Pim Visser, Frank Grosveld, Dies Meijer*

The POU transcription factor Oct-6, also known as SCIP or Tst-1, has been implicated as a major transcriptional regulator in Schwann cell differentiation. Microscopic and immunohistochemical analysis of sciatic nerves of Oct-6^{-/-} mice at different stages of postnatal development reveals a delay in Schwann cell differentiation, with a transient arrest at the promyelination stage. Thus, Oct-6 appears to be required for the transition of promyelinating cells to myelinating cells. Once these cells progress past this point, Oct-6 is no longer required, and myelination occurs normally.

Schwann cells are involved in the trophic support and insulation of axons and are the only glial cell type in peripheral nerve trunks. The two types of Schwann cells, myelinating Schwann cells associated with axons greater than 1 µm in diameter and nonmyelinating cells associated with multiple lower caliber axons, both differentiate from neural crest-derived Schwann cell precursors. Myelination initiation correlates

with axon diameter and is governed by axonal signals that are as yet not understood (1).

A number of transcription factors have been proposed to be involved in Schwann cell differentiation and myelination (2). Prominent among those is the POU domain transcription factor Oct-6 (also known as SCIP or Tst-1) (3). The Oct-6 protein is expressed in the Schwann cells of the sciatic nerve and the sympathetic trunk from embryonic day 16 (E16) onward (4). During postnatal nerve development, the expression of Oct-6 mRNA is gradually down-regulated and extinguished, with only spo-

Medical Genetics Center, Department of Cell Biology and Genetics, Erasmus University, Post Office Box 1738, 3000 DR Rotterdam, Netherlands.

*To whom correspondence should be addressed. E-mail: meijer@gen.tgg.eur.nl